Z. Phys. Chem. **217** (2003) 1169–1191
© by Oldenbourg Wissenschaftsverlag, München

Pressure and Temperature Dependence of the Decomposition Rate of Aliphatic *tert*-Amyl Peroxyesters

By Michael Buback*, Dorit Nelke, and Hans Peter Vögele

Institut für Physikalische Chemie der Georg-August-Universität, Tammannstraße 6, D-37077 Göttingen, Germany

Dedicated to Prof. Dr. Dr. h.c. mult. H. Gg. Wagner on the occasion of his 75th birthday

(Received June 18, 2003; accepted July 1, 2003)

Peroxides / Chemical Kinetics / Spectroscopy, Infrared / High Pressure

Thermal decomposition of several aliphatic *tert*-amyl (TA, 1,1-dimethylpropyl) peroxyesters, RC(O)OOTA, has been studied in dilute solution of *n*-heptane at pressures up to 2500 bar and temperatures up to 195 °C. The peroxides under investigation were: *tert*-amyl peroxyacetate (TAPA), *tert*-amyl peroxy-*n*-butanoate (TAPnB), *tert*-amyl peroxy-*iso*-butanoate (TAPiB, TA peroxy-2-methyl propionate), *tert*-amyl peroxy-2-ethylhexanoate (TAPO), and *tert*-amyl peroxypivalate (TAPP, TA peroxy-2,2-dimethyl propionate). The experiments were carried out in a tubular reactor at residence times up to 140 s. Peroxide concentration was monitored under continuous flow conditions via quantitative FT-IR spectroscopic analysis in an optical high-pressure cell positioned behind the tubular reactor. First-order decomposition kinetics over several half-lives were observed. For each TA peroxyester, rate equations for the first-order rate coefficient, $k_{obs}(p, T)$, are presented. k_{obs} values for TA peroxyester decomposition are by $23 \pm 9\%$ per cent above the corresponding numbers reported [1, 2] for associated *tert*-butyl (TB) peroxyesters, with the same R group and at identical p, T, and solvent environment. The carbon atom of the R moiety that is in α-position to the carbonyl group controls decomposition kinetics. k_{obs} is smallest in cases where this particular C-atom is a "primary" one and is largest when it is "tertiary". The "primary" TA peroxyesters are associated with activation energies around 140 kJ mol^{-1} whereas the E_A's of the "secondary" and "tertiary" TA peroxyesters are around 130 und 120 kJ mol^{-1}, respectively. The activation volumes, $\Delta V^{\ddagger}_{obs}$, of the "secondary" and "tertiary" TA peroxyesters are in the narrow range of $\Delta V^{\ddagger}_{obs} = 3.0 \pm 1.5$ cm^3 mol^{-1}. The $\Delta V^{\ddagger}_{obs}$'s of the "primary" TA peroxyesters are above 8 cm^3 mol^{-1}. Within the limits of experimental accuracy, the activation parameters of TA peroxyester decomposition are identical to the corresponding quantities reported for the associated TB peroxyesters [1, 2]. The activation parameters suggest that "primary" aliphatic peroxyesters decompose via single-bond scission whereas the "secondary"

* Corresponding author. E-mail: mbuback@gwdg.de

and "tertiary" TA peroxyesters undergo concerted two-bond scission or extremely fast successive scission of the two bonds which latter two processes can not be distinguished on the timescale of the experiments. The mode of primary bond dissociation, via single-bond or via concerted two-bond scission, largely affects initiator efficiency in free-radical polymerization. The peroxide decomposition rate data measured in dilute solution of compressed *n*-heptane are useful for simulation and optimization of technical high-pressure ethene polymerizations.

1. Introduction

Modeling of ethene polymerizations that are carried out at temperatures and pressures up to 300 °C and 3000 bar, respectively, requires knowledge of the relevant rate coefficients under such extreme conditions. In addition to propagation, termination, and chain-transfer rates, decomposition rate coefficients of peroxides that are used as chemical initiators need to be precisely known. In preceding papers [1, 2], the thermal decomposition of *tert*-butyl peroxyesters (TB peroxyesters) has been studied in *n*-heptane solution up to 2500 bar and between 110 and 190 °C. The observed first-order decomposition rate coefficients, k_{obs}, largely differ in absolute value and in pressure and temperature dependence. *Tert*-butyl peroxyacetate (TBPA) and *tert*-butyl peroxypivalate (TBPP) turn out to be the archetypes of thermal peroxyester decomposition via single-bond and via concerted (or extremely fast successive) two-bond scission, respectively. Scheme 1 illustrates the decomposition pathways. Primary dissociation produces an acyloxy radical, R–C(O)O, and an alkyloxy radical OR′. Two mechanisms may be distinguished depending on the lifetime of the acyloxy radical. Mechanism (a) applies to peroxyester decompositions where the acyloxy radical is rather stable and thus recombination, out-of-cage diffusion, and slow decarboxylation may occur with the caged situation (a). Mechanism (b) refers to the limiting situation of very fast decarboxylation of the acyloxy radical with rate coefficient k^*_{diss}. Decarboxylation is considered to proceed at such high rate that, without ultra-high experimental time resolution, peroxyester decomposition may be looked upon as a concerted two-bond scission reaction as is indicated by the dotted arrow in Scheme 1, with instantaneous production of the caged situation (b) of three species: two free radicals, R and OR′, and the CO_2 molecule. The two radicals may undergo in-cage combination or disproportionation or may diffuse out of the cage.

It should be noted that, as kinetics is monitored via the peroxyester carbonyl mode, the complex kinetic situation associated with mechanism (a) affects the spectroscopic probe because of the recombination reaction which restores the peroxyester molecule. With mechanism (b) out-of-cage diffusion and radical combination are also occurring. These processes are, however, not seen by the peroxyester carbonyl mode as combination produces an ether molecule. Under typical polymerization conditions, the ether is not capable of dissociating into free radicals. Combination under the conditions of mechanism (b)

thus constitutes a loss channel for free radicals which goes with a reduction of initiator efficiency. Cage recombination of acyloxy and alkyloxy radicals according to mechanism (a), on the other hand, restores the peroxyester which may produce free radicals in a subsequent decomposition step. Mechanisms (a) and (b) thus may be associated with quite different initiator efficiencies for free-radical polymerization, as has been demonstrated for TB peroxyesters in a recent study [3].

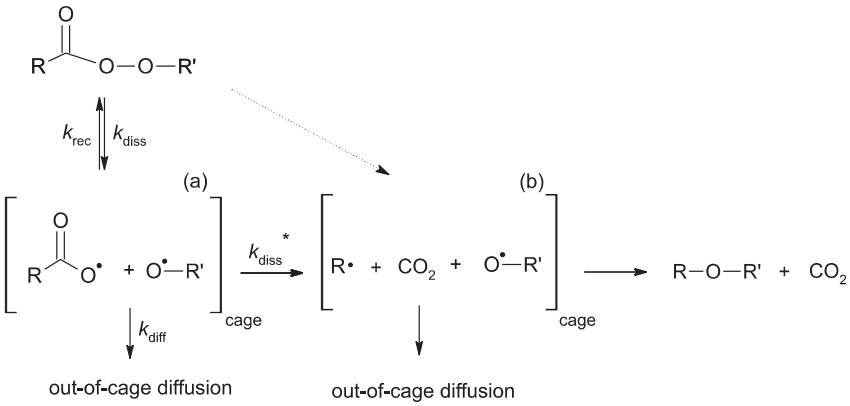

Scheme 1. Reaction scheme for the thermal decomposition of *tert*-amyl peroxyesters: mechanism (a) corresponds to situations where decomposition of the intermediate acyloxy radical is slow and recombination of the two "primary" radical species to the parent molecule may occur; mechanism (b) refers to almost instantaneous production, by very fast decarboxylation of the acyloxy radical, of radicals R and OR′ together with CO_2.

The studies into decomposition behavior of TBPA and TBPP revealed the crucial role of the carbon atom (in the acid-derived moiety R) that is in α-position to the carbonyl group. A tertiary such carbon atom in the so-called "tertiary" peroxyester TBPP favors concerted two-bond scission (mechanism (b)), as decarboxylation of the acyloxy radical produces a relatively stable *tert*-butyl radical and reduces the steric crowding at the tertiary carbon atom. With TBPA no significant steric crowding occurs at the particular α-carbon atom. Moreover, the relatively unstable CH_3 radical would be produced according to mechanism (b) which additionally disfavors this mechanism. Thermal TBPA decomposition thus proceeds by single-bond scission (mechanism (a)). Peroxides with a secondary carbon atom in α-position, so-called "secondary" peroxyesters with respect to the size of k_{obs} show an intermediate type of behavior, but with respect to the kinetic pathway decompose according to mechanism (b) as do the "tertiary" TB peroxyesters. The arguments presented for TB peroxy esters [1, 2] are in full agreement with the experimental material contained in the relevant literature [4–13].

For several reasons it appeared interesting to explore the decomposition kinetics of the related *tert*-amyl peroxyesters under high-pressure high-temperature conditions: (*i*) *Tert*-amyl peroxyesters differ from the *tert*-butyl compounds simply by replacing one methyl group in R' by an ethyl group. This small change should allow for a fine-tuning of initiator decomposition kinetics and efficiency. (*ii*) A successive decomposition step of the alkoxy radical OR (not shown in Scheme 1) to yield, via β-scission, an alkyl free radical and a ketone is more likely with *tert*-amyl than with *tert*-butyl peroxyesters. Thus the amount of oxygen-centered radicals should be lower with *tert*-amyl peroxyesters which in turn may affect in-cage reactivity and also out-of-cage chain-transfer activity of primary radicals.

The *tert*-amyl peroxyesters selected for the present study are listed in Table 1. With TAPA and TAPnB the carbon atom in α-position to the carbonyl group is a primary one. These compounds are referred to as "primary" TA peroxyesters. Along these lines, TAPiB and TAPO are "secondary" peroxyesters and TAPP is a "tertiary" peroxyester. TAPA, TAPO and TAPP are frequently used as initiators in technical polymerizations. The entire set of peroxides was kindly provided in high purity (see Table 1) by Akzo Nobel Polymer Chemicals. Among them, TAPnB and TAPiB were specially synthesized for our studies to allow for systematic investigations into the dependence of decomposition kinetics on the type of substituent R.

Among the peroxyesters in Table 1, rate coefficients have been published only for TAPP. They refer to decomposition in cumene solution at relatively low temperatures, 50 to 80 °C [14] and to decomposition in *iso*-dodecane between 120 and 200 °C at pressures up to 3000 bar [15, 16].

The aim of the present paper is to report experimental rate coefficients for decomposition of a series of *tert*-amyl alkyl peroxyesters, RC(O)OOTA, in dilute solution of *n*-heptane up to 2500 bar and partly up to 195 °C. Rate coefficients and the associated activation energy and activation volume parameters will be compared with the corresponding data reported for the decomposition of *tert*-butyl alkyl peroxyesters with identical acid-derived group R [1, 2].

2. Experimental section

The experiments were carried out under turbulent flow conditions in a continuously operated tubular reactor of 10 m length and 0.5 mm internal diameter. Both experimental set-up and procedure have already been detailed [1, 17]. Peroxide decomposition was monitored IR-spectroscopically via the carbonyl fundamental. A Bruker IFS 88 FT spectrometer equipped with a globar light source, a silicon-coated CaF_2 beam splitter, and a liquid-nitrogen-cooled MCT detector was used for IR analysis. The spectra were recorded in an optical high-pressure flow-through cell maintained at 50 °C. This cell is positioned directly

Table 1. *Tert*-amyl peroxyester, **R**–C(=O)–O–O–C(CH_3)$_2$(C_2H_5), under investigation.

R =	name	abbreviation	purity/wt.%
CH_3	*tert*-amyl peroxyacetate 1,1-dimethylpropyl peroxyacetate	TAPA	98.9
CH_2–CH_2–CH_3	*tert*-amyl peroxy-*n*-butanoate 1,1-dimethylpropyl peroxybutanoate	TAPnB	97.4
$CH(CH_3)_2$	*tert*-amyl peroxy-*iso*-butanoate 1,1-dimethylpropyl-peroxy 2-methylpropionate	TAPiB	97.9
$CH(C_2H_5)(C_4H_9)$	*tert*-amyl peroxy-2-ethylhexanoate 1,1-dimethylpropyl-peroxy 2-ethylhexanoate	TAPO	98.6
$C(CH_3)_3$	*tert*-amyl peroxypivalate 1,1-dimethylpropyl-peroxy 2,2-dimethyl-propionate	TAPP	97.1

behind the tubular reactor. Pressure is controlled within ± 15 bar and temperature to better than $\pm 0.5\,^{\circ}$C.

The peroxides were synthesized at the Akzo Nobel Polymer Chemicals Research Center Deventer in high purity (see Table 1). They were used as obtained as was the solvent *n*-heptane ($> 99\%$, Merck). The solutions were freshly prepared and air-liberated in-line using an HPLC solvent degasser. The initial peroxide concentration was always 1.0×10^{-2} M, which is sufficiently low to exclude induced decomposition. Further details about the experiments are given elsewhere [16].

3. Results

Measuring the rate coefficient of peroxide decomposition at a given pressure p and temperature T consists of recording IR spectra of the reaction solution after penetrating the tubular reactor at several residence times. Between 5 and 10 different flow rates, corresponding to different residence times of the turbulently flowing medium, were selected for deducing a single k_{obs} value. The spectra were taken at reaction pressure p, but at 50 °C. This lower temperature prevents further peroxide decomposition in the optical cell.

Illustrated in Fig. 1 is a spectral series collected during the decomposition of *tert*-amyl peroxypivalate (TAPP) at 500 bar and 115 °C. The intense

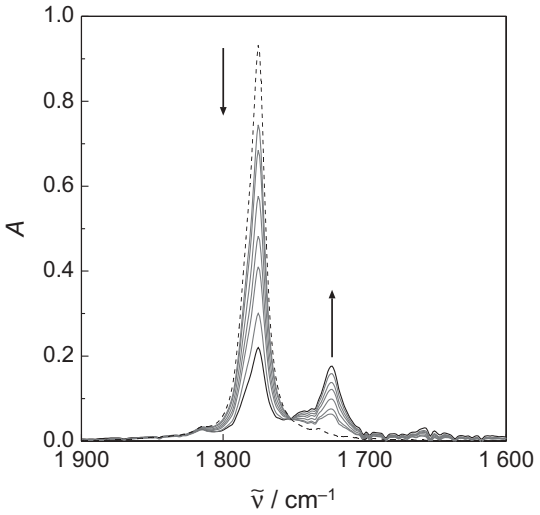

Fig. 1. Carbonyl region of the infrared absorbance spectrum measured during TAPP decomposition at 500 bar and 115 °C in *n*-heptane solution; initial peroxide (dashed line) concentration: 1.0×10^{-2} M; the arrows indicate the direction of spectral change with increasing residence time (black line for highest conversion).

carbonyl fundamental mode of TAPP at around 1774.5 cm^{-1} decreases toward larger residence (reaction) time. The growing absorption band close to 1722 cm^{-1} is due to acetone that is formed via β-scission of the intermediate *tert*-amyloxy free radical. The arrows indicate the direction of spectral change with (residence) time *t*. The spectra were taken up to a residence time of 140 s (black line with largest absorbance at 1722 cm^{-1}). The spectral series measured for the decay of the other peroxyesters (see Table 1) look rather similar with the band maximum positions of the carbonyl fundamentals however being slightly different as is illustrated by the data given in Table 2. The carbonyl peak position decreases in going from "primary" to "secondary" and to "tertiary" peroxyesters. Because of this shift toward lower wavenumbers, the carbonyl mode measured during TAPP decomposition exhibits stronger overlap with the carbonyl band of produced acetone than does the carbonyl mode of *tert*-amyl peroxyacetate (during decomposition of TAPA). The IR

Table 2. Peak position of the carbonyl fundamental mode of *tert*-amyl peroxyesters at ambient *p* and *T*.

peroxide	TAPA	TAPnB	TAPiB	TAPO	TAPP
$\tilde{\nu}_{max}/cm^{-1}$	1789.1	1785.7	1783.5	1779.7	1774.5

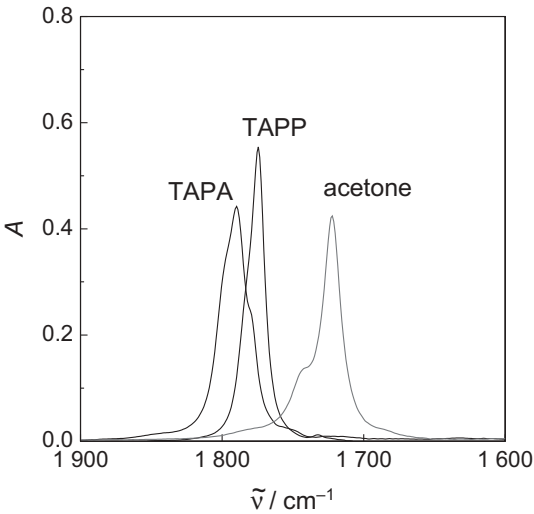

Fig. 2. Carbonyl region of the infrared absorbance spectra of TAPA, TAPP, and acetone in 0.01 M *n*-heptane solution.

carbonyl spectra of TAPA, TAPP, and acetone each in 0.01 molar solutions of *n*-heptane are shown in Fig. 2. The acetone spectrum refers to the hypothetical situation of complete decomposition of both peroxyesters and of the intermediate *tert*-amyloxy radical reacting exclusively, via β-scission, to acetone. As compared to the situation with *tert*-butyl peroxyesters, a significantly larger fraction of ketone is produced during *tert*-amyl peroxyester decomposition. To ensure that the acetone absorption does not invalidate the kinetic analysis carried out via the peroxyester carbonyl modes, the spectra measured during TA peroxyester decomposition were band-separated via a subtraction procedure that uses an acetone IR spectrum recorded in *n*-heptane at identical p and T. The fitting process which eliminates the contribution of acetone to overall absorption is carried out for the wavenumber region 1722 to 1660 cm^{-1}.

Peroxyester concentration is deduced from the integrated absorbance (after elimination of the contributions from acetone) for the narrow wavenumber region at 3.0 cm^{-1} to either side of the carbonyl peak maximum. At the fairly low peroxide concentrations employed within the present study and with the nonpolar solvent *n*-heptane, Beer-Lambert's law is valid and peroxyester concentration is proportional to the above-mentioned integrated absorbance measure. The IR method is perfectly suited for in-line kinetic analysis of peroxyester decay. It should be noted that monitoring peroxide decay rather than detecting product concentrations significantly enhances the quality of decomposition rate measurement. The procedure of deriving rate coefficients of peroxide decomposition is detailed elsewhere [17c,17d].

It should further be noted, that the decomposition reaction may also be monitored via an IR band at around 3620 cm^{-1} (not shown in Fig. 1) which is due to *tert*-pentanol that results from the hydrogen-abstraction reaction of the intermediate *tert*-amyloxy free radical. Alkanes, alkenes, and ethers which are also produced, via combination and disproportionation reactions of alkyl or alkyloxy free radicals (from decarboxylation of intermediate acyloxy radicals and from β-scission of intermediate alkyloxy radicals) may not be detected IR-spectroscopically for decompositions carried out in solution of *n*-heptane. The concentrations of these species are, however, accessible from gas chromatographic analysis of product mixtures after complete peroxide decomposition. The results of such GC analysis which contain a wealth of additional kinetic information will be presented in a forthcoming paper [18].

For decomposition reactions of TAPP at 500 bar and temperatures between 100 and 130 °C, the logarithm of relative peroxide concentration, $\ln(c_t/c_0)$, is plotted *vs*. residence (reaction) time t in Fig. 3. c_t refers to stationary peroxyester concentration after passing the tubular reactor at residence time t. c_0 is the initial peroxyester concentration at $t = 0$. Peroxyester conversion per unit reaction time largely increases with temperature. At 105 °C less than 50 per cent are decomposed after 120 s (50% conversion correspond to $\ln(c_t/c_0) = -0.69$) whereas at 130 °C a residence time of 70 s exceeds five decomposition half-lives. The $\ln(c_t/c_0)$ *vs*. t data recorded for each decomposition reaction (at constant p and T) closely fit to a straight line which demonstrates that decomposition kinetics is adequately described by a first-order rate law. The slope to each of these lines yields the observed (overall) first-order rate coefficient, k_{obs}:

$$\frac{dc}{dt} = -k_{obs}c \tag{1}$$

where c is peroxyester concentration.

Plots of the same quality as in Fig. 3 are obtained for each of the peroxides listed in Table 1. The first-order decomposition rate coefficients, k_{obs}, derived from the straight line $\ln(c_t/c_0)$ *vs*. t plots are summarized in Tables 3 and 4. Given in Table 3 are the rate coefficients of TAPA, TAPnB, TAPiB, TAPO, and TAPP decomposition in solution of *n*-heptane at 500 bar and temperature variation. The TAPP data set marked with an asterisk is from discontinuous experiments carried out by Sderra [19] in a stainless steel batch reactor. This data is in satisfactory agreement with the values from the present study measured in the tubular reactor. Results for the pressure dependence of k_{obs} at constant decomposition temperature are summarized in Table 4. The multiple entries for 500 bar result from the fact that the temperature dependence of k_{obs} has been studied at this pressure. Thus data is available from measuring pressure dependence at constant temperature and from measuring temperature dependence at 500 bar. The data from

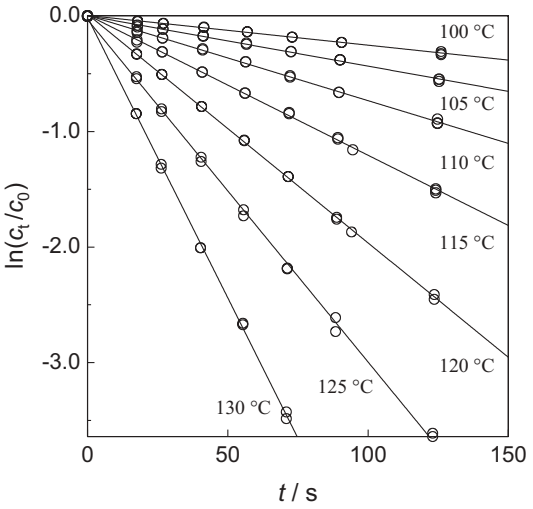

Fig. 3. Time dependence of relative peroxyester concentration, $\ln(c_t/c_0)$, of TAPP decomposition in *n*-heptane solution at 500 bar and temperatures between 100 and 130 °C.

Table 3. First-order rate coefficients, k_{obs}, for the thermal decomposition of *tert*-amyl peroxyesters in *n*-heptane solution at various temperatures and 500 bar (* data obtained in a stainless steel batch reactor [19]).

	$k_{obs}/10^{-3}$ s^{-1} (500 bar)					
T/°C	TAPA	TAPnB	TAPiB	TAPO	TAPP	TAPP*
100					2.57	2.70
105					4.36	
110					7.39	8.70
115					12.1	
120					19.8	19.8
125			2.65	5.07	29.6	
130			4.33	8.41	48.6	50.5
135			7.00	13.3		
140			11.5	22.1		130
145		3.27	17.9	35.3		
150	4.62	5.34	28.2	52.5		
155	7.72	8.38	43.2	80.0		
160	11.8	13.3				
165	18.4	21.2				
170	29.6	32.8				
175	45.7	48.6				
180	67.0	76.8				
185	101					

Table 4. First-order rate coefficients, k_{obs}, for the thermal decomposition of *tert*-amyl peroxyesters in *n*-heptane solution measured as a function of pressure at constant temperature (*data obtained in a stainless steel batch reactor [19]).

	$k_{obs}/10^{-3}\ s^{-1}$						
p/bar	TAPA 170 °C	TAPnB 170 °C	TAPnB 160 °C	TAPiB 145 °C	TAPO 140 °C	TAPP 120 °C	TAPP* 120 °C
100							21.1 21.0
200			14.5				
250	31.8						
300		32.0		18.2 18.8			20.4
400	29.9						
500	29.1 29.6	32.5 32.8	13.2 13.3	19.0 18.3 17.9	22.6 22.1	19.1 19.4 19.8	19.8 19.8
600	28.1						
750		30.6					20.1
800	26.4						
1000	24.4	28.8	12.4	17.7 17.7	21.5	18.3	20.5
1500	20.7	25.2	10.8	17.0 17.2	20.2	17.5	20.4
2000	17.4	22.5	9.9	15.7 16.3	19.0	17.2	18.2 17.9
2500	13.4	19.2	8.4	14.0 14.4	16.5	14.9	

the completely independent experimental series is in very satisfactory agreement. As can be seen from the entries in Tables 3 and 4, k_{obs} is strongly enhanced with increasing temperature, but is weakly reduced toward higher pressure. The accuracy of k_{obs} is estimated to be better than $\pm 10\%$. Within each series of experiments, on the same peroxide at either constant temperature or constant pressure, the precision should be even higher, probably close to $\pm 5\%$.

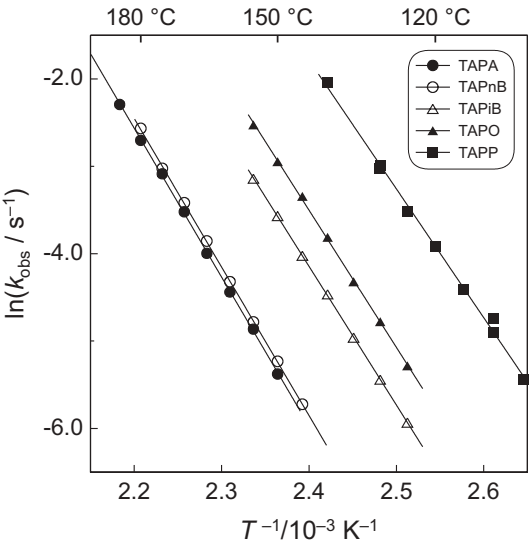

Fig. 4. Temperature dependence of k_{obs} for *tert*-amyl peroxyester decomposition at 500 bar, the circled symbols refer to "primary", the triangled symbols to "secondary" and the squared symbols to "tertiary" TA peroxyesters.

Presented in Fig. 4 are Arrhenius plots of k_{obs} for 500 bar. The circles refer to "primary" TA peroxyesters, the triangles to "secondary" and the squares to "tertiary" TA peroxyesters. For each peroxide, the k_{obs} values closely fit onto an Arrhenius straight line. As has been seen for *tert*-butyl peroxyester [1, 2] the k_{obs} values for the two "primary" peroxyesters, TAPA and TAPnB, are almost identical. From linear regression of ln k_{obs} *vs*. T^{-1} data, the activation energy, E_A, and the pre-exponential factor, A, are obtained. Both Arrhenius parameters are listed for the entire set of TA peroxyesters in Table 5. The activation energy increases from "tertiary" to "secondary" and to "primary" TA peroxyesters, as does the pre-exponential factor.

Literatures values of activation energies have only been reported for TAPP with this data referring to decompositions in solution of cumene [14] and of *iso*-dodecane [15, 16]. The activation energy deduced, via $E_A = \Delta H^{\neq} + RT$, from the activation enthalpy, $\Delta H^{\neq}$, reported by Komai *et al.* [14] is $E_A = 117.7 \pm 1.3\ \mathrm{kJ\,mol^{-1}}$. Within the limits of experimental accuracy and taking into account that different solvents have been used in the two investigations, this number is close to what has been observed in the present study: $E_A = 122.5 \pm 3.5\ \mathrm{kJ\,mol^{-1}}$. The value reported by Luft *et al.* [15] $E_A = 113\ \mathrm{kJ\,mol^{-1}}$ from experiments in *iso*-dodecane solution is, however, clearly below the number deduced from our measurements.

Plotted in Fig. 5 is the pressure dependence of ln k_{obs} for the entire set of TA peroxyesters. Inspection of ordinate scales in Figs. 4 and 5 tells that effects

Table 5. Pre-exponential factor, A, and activation energy, E_A, of the decomposition rate coefficient, k_{obs}, of *tert*-amyl peroxyesters in *n*-heptane solution; the reaction pressure and the temperature range of the experiments are listed.

peroxide	p/bar	T/°C	$A \times 10^{-14}$/s^{-1}	E_A/kJ mol^{-1}
TAPA	500	150–185	14.8	141.7 ± 3.0
TAPnB	500	145–180	15.1	141.3 ± 3.0
TAPiB	500	125–155	5.83	132.1 ± 3.0
TAPO	500	125–155	7.27	130.7 ± 3.0
TAPP	500	100–140	3.83	122.5 ± 3.5

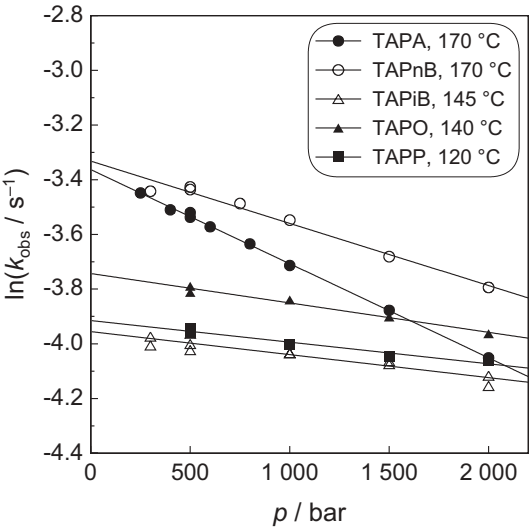

Fig. 5. Pressure dependence of k_{obs} for *tert*-amyl peroxyesters at constant temperatures (between 120 and 170 °C); the circle symbols refer to "primary", the triangle symbols to "secondary" and the square symbols to "tertiary" TA peroxyesters.

on ln k_{obs} resulting from the application of pressures up to a few kbar are minor as compared to changes resulting from varying temperature by about 30 °C. In order to precisely measure such small pressure-induced changes, the experiments for a particular peroxyester had to be carried out at a temperature which is very suitable for the specific compound. The pressure dependence of k_{obs} is more pronounced for the "primary" than for the "secondary" and "tertiary" TA peroxyesters. A weak curvature that has been seen with the "primary" *tert*-butyl peroxyesters can not be detected with TAPA and TAPnB. Activation volumes, $\Delta V^{\ddagger}_{obs}$, are determined from the slope to the linear ln k_{obs} *vs.* p

Table 6. Activation volume, $\Delta V^{\neq}_{obs}$, of the decomposition rate coefficient, k_{obs}, of *tert*-amyl peroxyesters determined in continuous-flow experiments in *n*-heptane solution; the reaction temperature and the pressure range of the experiments are listed.

peroxide	T/°C	p/bar	$V^{\neq}_{obs}$/cm^3 mol^{-1}
TAPA	170	250–2000	12.7 ± 1.0
TAPnB	160	200–2500	8.1 ± 0.6
TAPnB	170	300–2000	8.4 ± 0.6
TAPiB	145	300–2000	2.9 ± 1.1
TAPO	140	200–2000	3.7 ± 1.5
TAPP	120	500–2000	2.6 ± 0.6

correlations according to Eq. (2):

$$\left(\frac{\partial \ln k_{obs}}{\partial p}\right)_T = -\frac{\Delta V^{\neq}_{obs}}{RT}. \tag{2}$$

The resulting activation volumes are listed in Table 6. The numbers for the "primary" TA peroxyesters clearly exceed the numbers deduced for "secondary" and "tertiary" TA peroxyesters.

Only for TAPP a literature value of $\Delta V^{\ddagger}_{obs}$ has been reported [15, 16]: The number provided for TAPP decomposition in *iso*-dodecane, $\Delta V^{\ddagger}_{obs} = 9.4$ cm^3 mol^{-1}, is however in conflict with the much smaller activation volume, $\Delta V^{\ddagger}_{obs} = 2.6 \pm 0.6$ cm^3 mol^{-1}, determined within the present study. Because of the close similarity of our number with the activation volume determined for TBPP [1] we consider our $\Delta V^{\ddagger}_{obs}$ to be reliable.

4. Discussion

First-order kinetics, with rate coefficient k_{obs}, adequately represents decomposition rate in dilute solution of *n*-heptane over several half-lives for the entire set of TA peroxyesters. As peroxyester concentration is well above peroxide concentrations occurring during free-radical polymerization, the measured rate coefficients should be well suited for modeling thermal peroxyester decomposition in technical polymerizations, at least of non-polar monomers such as ethene. Because of the strong application-oriented interest in such decomposition rate data, equations for k_{obs} should be given which allow for estimates of k_{obs} in hydrocarbon solution at arbitrary p and T conditions within the range of the underlying experiments and perhaps even at some modest extrapolation beyond this range.

Along the lines applied for modeling TB peroxyester decomposition rate [2], the Arrhenius-type expression, Eq. (3), has been used for fitting $k_{obs}(p, T)$ data. Applying Eq. (3) rests on the following two assumptions:

(*i*) the pre-exponential factor is independent of p and T and (*ii*) the activation volume is independent of temperature. The expression for k_{obs}/s^{-1} (with p in bar and T in K) reads:

$$k_{obs}(p, T)/s^{-1} = A \exp\left(\frac{E_A(0\,\text{bar}) + \Delta V^{\neq}\, p/\text{bar}}{RT/\text{K}}\right) . \quad (3)$$

The constants A, E_A (0 bar) and $\Delta V^{\neq}$, which are characteristic quantities for a particular peroxyester, are listed in Table 7. The units for p and R are chosen such that the product terms $\Delta V^{\neq} p$ and RT are in kJ mol^{-1}.

A, E_A (0 bar) and $\Delta V^{\neq}$ have been found by least squares fitting (with the Microsoft Excel Solver function) of the available experimental rate coefficients to Eq. (3). The number of k_{obs} data points, N, which has been subjected to the fitting procedure is listed for each TA peroxyester. Also given in Table 7 are the maximum pressure and the temperature range of the underlying experiments. From Eq. (3), decomposition rate coefficients, k_{obs}, have been calculated for the experimental p and T conditions. The maximum relative deviation, $(|\Delta k|/k)_{max}$, of the so-obtained (calculated via Eq. (3)) k_{obs} values from the associated experimental values is 14.2% for one data point out of the TAPP experimental series (Table 7). The average deviation of calculated and measured rate coefficients for this series, $(|\Delta k|/k)_{av}$, is 3.5%. For the other TA peroxyesters smaller maximum and average deviations between experimental and calculated k_{obs} are seen. Mostly, as is indicated by the entries in Table 7, $(|\Delta k|/k)_{max}$ is below 5% and $(|\Delta k|/k)_{av}$ is below 2% which demonstrates that Eq. (3) provides an adequate fit of the measured k_{obs} data. Eq. (3) thus should be suitable for estimating k_{obs} in the pressure and temperature range covered by the underlying experiments. As Eq. (3) has a clear physical basis, it appears justified to use this equation (with the parameters given in Table 7) also for modest extrapolation beyond the experimental p and T range, *e.g.*, for conditions met in high-pressure ethene polymerization.

Prior to a discussion of the temperature and pressure dependence of k_{obs}, it appears rewarding to compare k_{obs} values of *tert*-butyl and *tert*-amyl peroxyesters with a common acid-derived R group, *e.g.*, decomposition rate coefficients of TBPA with the ones of TAPA and k_{obs} of TBPP with k_{obs} of TAPP for identical p, T, and solvent environment. For each of the five types of TA peroxyesters (acetate, *n*-butanoate, *iso*-butanoate, 2-ethyl hexanoate (octanoate), and pivalate) investigated within the present paper, $k_{obs}(p, T)$ data of the associated TB peroxyester have recently been reported [1, 2]. The comparison is made by calculating, for the total of 90 TA peroxyester k_{obs} values deduced from independent tubular reactor experiments, the associated TB peroxyester k_{obs} value from the rate expressions reported in Ref. [1, 2]. Plotted in Fig. 6 is the integral distribution of experimental data points, ΣN, as a function of the percentage difference, $100(k_{TA} - k_{TB})/k_{TA}$,

Table 7. Parameters A, $E_A(0\,\text{bar})$ and $\Delta V^{\neq}$, referring to Eq. (3). The numbers are obtained by non-linear least squares fitting of the experimental k_{obs} values.

	A/s^{-1}	$E_A(0\,\text{bar})/$ kJ mol^{-1}	$\Delta V^{\neq}/$ cm^3 mol^{-1}	N	$\left(\frac{\lvert\Delta k\rvert}{k}\right)_{max}$	$\left(\frac{\lvert\Delta k\rvert}{k}\right)_{av}$	$p_{max}/$ bar	temperature range/°C
TAPA	1.52×10^{15}	141.2	12.5	16	2.4	1.1	2000	150–185
TAPnB	1.03×10^{15}	139.6	8.2	20	5.1	1.8	2500	145–180
TAPiB	7.53×10^{14}	132.9	2.6	17	4.4	1.6	2000	125–155
TAPO	7.27×10^{14}	130.5	2.8	11	3.6	2.2	2000	125–155
TAPP	4.11×10^{14}	122.7	2.4	26	14.2	3.5	2000	100–140

between pairs of k_{obs} values for TA and TB peroxyesters under otherwise identical conditions including the same type of acid-derived R group. ΣN indicates the total number of data points for which the percentage difference between associated TA and TB peroxyesters k_{obs} is $100(k_{TA} - k_{TB})/k_{TA}$ or below.

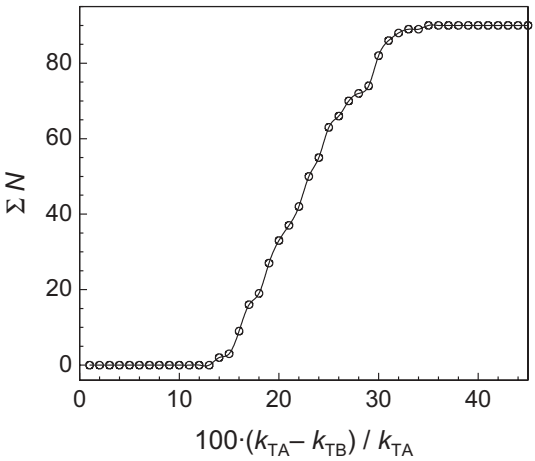

Fig. 6. Comparison of decomposition rate coefficients for associated TA and TB peroxyesters. The sum of experimental data points, ΣN, is plotted *vs*. relative deviation (see text).

Within the wide pressure and temperature range and for the five types of acid functionalities, the TA rate coefficients are always above k_{obs} of the associated TB peroxyester. It should be noted that the observed enhancements of k_{obs} in going from the TB to the associated TA peroxyester occur within the narrow range from 14 to 32%, which corresponds to a mean enhancement by $23 \pm 9\%$ for the entire experimental data set. The scattering appears to be not overly large in view of the fact, that uncertainties of rate coefficients measured for TA and TB systems may add or may compensate each other. The difference in TA and TB rate coefficients is more or less equally distributed around the mean value for the acetates, *iso*-butanoates, octanoates, and pivalates. With the *n*-butanoates, the difference is systematically higher, which effect leads to the weak sigmoidal curvature at $100(k_{TA} - k_{TB})/k_{TA}$ values around 30%. Whether or not this effect is due to specific characteristics of either the TA or TB peroxy-*n*-butanoate samples or due to some experimental imperfection is difficult to decide, in particular as the observed discrepancy is rather small. For peroxypivalates a higher decomposition rate coefficient of TAPP as compared to TBPP under otherwise identical reaction conditions has also been reported in the literature. Komai *et al.* [14] found a difference of 16% whereas the data presented by Luft *et al.* [15, 16] suggest k_{obs} of TAPP to be only by 12% above the associated TBPP value. The reason for k_{obs} of TA peroxyesters being above the associated k_{obs} values of the TB compound by about the same percentage, as is indicated by the entire body of our k_{obs} data, will be addressed further below after discussion of activation energies and activation volumes.

Temperature and pressure dependence of k_{obs}

Activation energy provides insight into decomposition mechanisms. With respect to the systems under investigation, it needs to be noted that, according to Scheme 1, the k_{obs} values are overall quantities to which elementary reaction steps such as dissociation, (re)combination, out-of-cage diffusion, and decarboxylation are contributing. On the other hand, the activation energy of k_{obs}, E_A, will certainly be dominated by the primary dissociation step.

Contributions of fast (or even instantaneous) decarboxylation to E_A may be detected from so-called Polanyi plots, in which $E_A(k_{obs})$ is plotted *vs*. C–H bond dissociation energy (*BDE*) of the associated hydrocarbon molecule R–H in which R is the free-radical moiety that is characteristic for the associated acid-derived functionality. This type of analysis assumes a proportionality of activation energy and of reaction heat for the same type of transformations being carried out for similar components preferably within homologous series [20]. The procedure has already been tested for the decomposition of a variety of TB peroxyesters, RC(O)OOTB, by Engel *et al.* [21], in our previous paper [2] and, even more recently, in the dissertation of Sandmann [22]. *BDE*(R–H) serves as a measure of the stability of the free radical R. A linear E_A *vs*. *BDE*(R–H) correlation with slope unity indicates that the stability of R significantly affects the rate determining step which in turn strongly suggests a close-to-concerted two-bond scission mechanism. In case that the R–C(O)O bond is not or not immediately broken during peroxyester decomposition, the specific type of R group is less important as bonds other than the one in α-position to the carbonyl group are too far from the O–O reaction site to be of significant influence on the kinetics. Such peroxides which exclusively undergo single-bond scission are expected to exhibit activation energies that are independent of *BDE*(R–H). Moreover, for this class of peroxyesters even absolute k_{obs} values at identical p, T, and solvent environment are close to each other (see [22] and Fig. 4).

The R–H bond dissociation energy was deduced as the enthalpy of the reaction

$$\mathrm{R{-}H} \xrightarrow{\Delta_r H} \mathrm{R\cdot} + \mathrm{H\cdot}\ .$$

using the Benson procedure [23] for estimating the standard heat of formation of R and R–H. For consistency reasons, estimated values were also used in cases where experimental values are available [24]. The standard heat of formation of H was taken from Cox and Bilcher [25]. The estimates of *BDE*(R–H), in principle, are restricted to species in the dilute gaseous phase. Errors associated with applying this data to reactions in hydrocarbon solution should, however, not markedly affect the Polanyi plot, as the same procedure is used for deducing *BDE*(R–H) of the entire set of R–H compounds. The activation energy, E_A, that is used for the Polanyi plot refers to zero pressure.

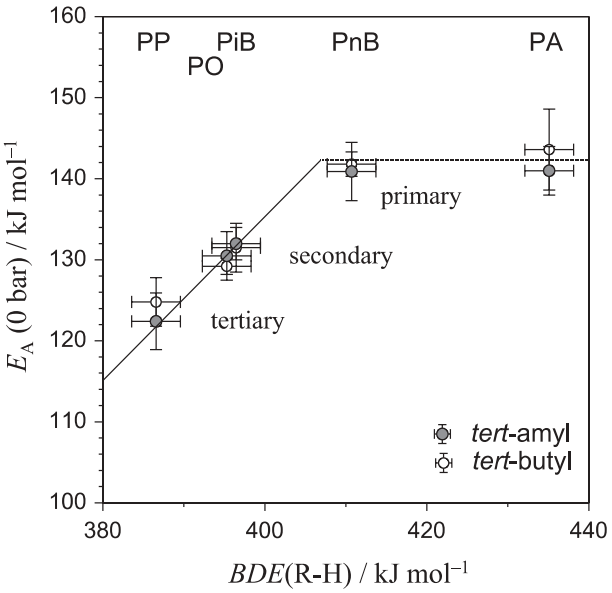

Fig. 7. Activation energy, E_A, of the decomposition rate coefficient, k_{obs}, for *tert*-amyl (filled circles) and *tert*-butyl (open circles) peroxyesters, plotted *vs*. the bond dissociation energy of the associated alkane, *BDE*(R–H).

Fig. 7 shows the E_A(0 bar) *vs*. *BDE*(R–H) plot for the aliphatic TA peroxyesters of the present work (full circles) together with the data for the corresponding TB peroxyesters (open circles) from [22]. As within the preceding paper on the TB peroxyesters [22], a straight line with slope unity has been used to fit the data for the "secondary" and "tertiary" peroxyesters. The "primary" peroxyesters are fitted by a horizontal line. Actually the line with slope unity is the same as used for the TB peroxyesters alone. The horizontal line is by about 1.5 kJ mol^{-1} below the line given in Ref. [22], which difference however, is within the limits of experimental accuracy. Inspection of the activation energies in Fig. 7 tells, that the numbers for associated TA and TB peroxyesters, within experimental accuracy, must be considered identical. Actually, for three out of five pairs of activation energies the data are overlapping within the small size of the symbols. The minor change of replacing one methyl group on the *tert*-butyloxy moiety by an ethyl group, to yield *tert*-amyloxy, does not affect E_A to any measurable extent. As a consequence, the same arguments with respect to the mode of bond scission do apply to both TA and TB peroxyesters: The "primary" peroxyesters, *e.g.*, the peroxy-*n*-butanoates and peroxyacetates, undergo single-bond scission, whereas the "secondary" and "tertiary" peroxyesters show characteristics of concerted two-bond scission which may be best understood in terms of decomposition with

an extremely short-lived intermediate R–C(O)O that almost instantaneously undergoes decarboxylation [26].

The application of high pressure toward identifying the mechanism of peroxide decomposition reactions has been pioneered by Neuman *et al.* [11, 12]. Activation volumes up to $4\,cm^3\,mol^{-1}$ have been assigned to concerted two-bond scission and numbers around $10\,cm^3\,mol^{-1}$ to single-bond scission. Neuman and Amrich [12] explained the larger value of $\Delta V^{\ddagger}_{obs}$ in case of single-bond scission by additional contributions (to $\Delta V^{\ddagger}_{obs}$) resulting from the pressure dependence of out-of-cage diffusion of the geminate free radicals. Based upon their expression, Eq. (4) [12], the dependence of $\ln k_{obs}$ on p for several primary peroxyesters undergoing single-bond scission was modeled in the previous paper [2].

$$k_{obs} = k_{diss}\left(\frac{k_{diff} + k^{*}_{diss}}{k_{diff} + k^{*}_{dis} + k_{rec}}\right) \tag{4}$$

k_{diss}, k_{rec}, k_{diff}, and k^{*}_{diss} (see Scheme 1) are the rate coefficients of peroxide bond dissociation, of recombination of the primary free radicals, of out-of-cage diffusion (of at least one) of these primary radicals, and of decarboxylation of the acyloxy radical, respectively. Eq. (4) allows for representing and predicting reasonable values of activation volume, $\Delta V^{\neq}$, of "primary" TB peroxyesters [2]. In addition, the very weak curvature of $\ln k_{obs}$ *vs*. p data observed for primary TB peroxyesters can be modeled via Eq. (4). This curvature appears to be essentially due to the pressure dependence of k_{diff}, that is of out-of-cage diffusion of one or both of the primary products from peroxyester decomposition. No clear indication of such a curvature is seen with the primary TA peroxyesters. So far, it is not clear whether this curvature does not occur or whether it is too weak to be unambiguously detected.

In Fig. 8, the pressure dependence of decomposition rate of three types of TA and TB peroxyesters, peroxy-*n*-butanoates, peroxy-*iso*-butanoates, and peroxypivalates is compared. They are examples of "primary", "secondary", and "tertiary" peroxyesters, respectively. In order to allow for easier comparison of the data taken at different temperatures, reduced k_{obs} is plotted in an $\ln[k_{obs}/k_{obs}(2000\,bar)]$ *vs*. pressure diagram, thus taking the respective k_{obs} values at 2000 bar as the reference. The TA peroxyester data is represented by full symbols and the TB data by open symbols. The $k_{obs}/k_{obs}(2000\,bar)$ data points for peroxyesters referring to the same R group almost coincide, which observation indicates that, in addition to the temperature dependence, also the pressure dependence of k_{obs} is not significantly affected in going from the *tert*-butyl to the associated *tert*-amyl peroxyester. As a consequence, the arguments deduced from the pressure dependence of k_{obs} for TB peroxyesters should also apply to TA peroxyesters: The relatively small activation volumes, $\Delta V^{\ddagger}_{obs} = 3.0 \pm 1.5\,cm^3\,mol^{-1}$, observed for the "secondary" (*iso*-butanoates) and "tertiary" (pivalates) peroxyesters are indicative of very fast sequential

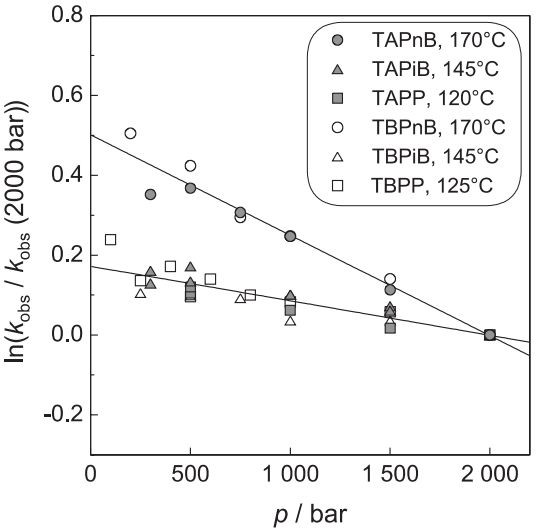

Fig. 8. Pressure dependence of relative (with respect to the calculated 2000 bar value) rate coefficients for *tert*-amyl (filled symbols) and *tert*-butyl (open symbols) peroxyesters at constant temperatures (between 120 and 170 °C).

decomposition which, on the timescale of the present experiments, closely resembles concerted two-bond scission. The "primary" peroxyesters, TBPnB and TAPnB, on the other hand show a pronounced pressure dependence, with activation volumes around $\Delta V^{\ddagger}_{obs} = 10 \pm 2\ cm^3\ mol^{-1}$, as are expected for peroxyesters undergoing single-bond scission. An important point to note is that measuring the pressure dependence indeed provides valuable mechanistic information. Thus a clear distinction in decomposition behavior of *iso*- and *n*-butanoates can be made. The Polanyi plot (Fig. 7), which rests on measuring k_{obs} (only) as a function of temperature, does not allow for a decision whether the peroxy-*n*-butanoates undergo single-bond scission, represented by the horizontal line, or two-bond scission, represented by the straight line with slope unity.

The close similarity in activation parameters of k_{obs} for associated TA and TB peroxyesters indicates that differences in the pre-exponentials are responsible for k_{obs} of TA peroxyesters exceeding k_{obs} of the corresponding TB. That the rate coefficients differ by approximately the same percentage, may be taken as an indication for the primary step, as illustrated in Scheme 1, being indeed similar for the different types of acid functionalities R. The higher k_{obs} values seen with the TA peroxyesters may be due to the fact that, within the transition structure of the TA compounds, the *tert*-amyloxy moiety experiences a larger degree of motional freedom with respect to the parent molecule than does the *tert*-butoxy moiety with respect to the parent

TB peroxyester. As a consequence, the partition function term for transition structures of TA peroxyesters is enhanced to a larger extent than is the case with TB peroxyesters, which is consistent with higher pre-exponentials of TA peroxyesters. This tentative explanation needs to be supported by quantum-chemical calculations and by additional experiments on peroxyesters where steric hindrance is further enhanced by introducing bulky alkoxy moieties.

The observation that k_{obs} of TA peroxyesters is by one and the same percentage, of about $23 \pm 9\%$, above the value of the associated TB peroxyester under otherwise identical conditions is extremely useful as k_{obs} data is available for a wide variety of TB peroxyesters. This data may thus serve as a basis for estimates of k_{obs} for TA peroxyesters that have not been experimentally studied so far. Moreover, it appears interesting to investigate, whether also for other *tert*-alkyl moieties such simple correlations hold which might enable k_{obs} estimates on the basis of characteristic percentage differences. Such differences would be made available from a very few kinetic investigations into decomposition kinetics of peroxyesters with a particular *tert*-alkyloxy moiety. Having access to a large number of measured and estimated k_{obs} values is important for designing and optimizing technical polymerizations with special interest in the high-pressure ethene polymerization. The molecular environment of dense ethene-polyethylene mixtures, as are occurring during this high-pressure process, appears to be sufficiently close to the environment provided by pressurized *n*-heptane. This is indicated by the excellent suitability of the rate coefficients for TB peroxyester decomposition, from studies in *n*-heptane, toward analysis of ethene polymerization kinetics and, in particular, of initiation efficiencies of these peroxyesters [3].

Varying the type of *tert*-alkoxy moiety, in addition to changing k_{obs}, may have a significant effect on the type of produced primary free radicals. As has been mentioned above, decomposition of TA peroxyesters results in a larger extent of ketone formation than observed with TB peroxyesters. The reason behind this effect is that β-scission of *tert*-amyloxy radicals occurs much faster than with *tert*-butyloxy radicals. This clear difference between TA and TB peroxyesters may affect cage reactions and thus initiator efficiency in free-radical polymerization. These aspects are currently under investigation.

5. Concluding remarks

Overall rate coefficients, k_{obs}, of decomposition in *n*-heptane have been determined for several aliphatic TA peroxyesters within wide ranges of pressure and temperature. Irrespective of the type of acid-derived moiety R, the rate coefficients of TA peroxyesters are by about 23% above k_{obs} of the associated TB peroxyester. This difference is assigned to an enhancement of the pre-exponential factor for TA peroxyesters, as both activation energy and activation volume

are identical for associated TA and TB peroxyesters. The activation parameters suggest that "primary" peroxyesters, such as peroxyacetates and peroxy-*n*-butanoates, decompose via single-bond scission to primary free radicals that may recombine to restore the parent peroxyester molecule. "Secondary" peroxyesters, such as peroxy-*iso*-butanoates and peroxy-2-ethyl-hexanoates, and "tertiary" peroxyesters, such as peroxypivalates, on the other hand, undergo very rapid decarboxylation of the intermediate carbonyloxy radical which, on the timescale of the present experiments, suggests a concerted two-bond scission process. The reported data should be well suited for analysis of TA peroxyester efficiency in high-pressure ethene polymerization.

Acknowledgement

The authors are grateful to the Deutsche Forschungsgemeinschaft for financial support of this study within the Sonderforschungsbereich 357 ("Molekulare Mechanismen unimolekularer Prozesse"). The intense cooperation enjoyed with Akzo Nobel Polymer Chemicals, in particular with Dr. B. Fischer, Dr. F. J. Hoogesteger, Dr. J. Meijer, Dr. A. Van Swieten, and R. Gerritsen, is gratefully acknowledged, as is the synthesis and provision of the peroxide samples. Further support has been provided by the Fonds der Chemischen Industrie.

References

1. M. Buback, S. Klingbeil, J. Sandmann, M.-B. Sderra, H. P. Vögele, H. Wackerbarth, and L. Wittkowski, Z. Phys. Chem. **210** (1999) 199.
2. M. Buback and J. Sandmann, Z. Phys. Chem. **214** (2000) 583.
3. P. Becker, M. Buback, and J. Sandmann, Macromol. Chem. Phys. **203** (2002) 2113.
4. Y. Sawaki, in *Organic Peroxides*, W. Ando (Ed.), John Wiley and Sons, New York (1992) 425.
5. T. Koenig, in *Free Radicals*, Vol. I, J. K. Kochi (Ed.), Wiley-Interscience, New York (1973) 113.
6. P. D. Bartlett and R. R. Hiatt, J. Am. Chem. Soc. **80** (1958) 1398.
7. W. Pryor and K. Smith, Int. J. Chem. Kin. **3** (1971) 387.
8. T. Koenig and R. Wolf, J. Am. Chem. Soc. **89** (1967) 2948.
9. T. Koenig, J. Huntington, and R. Cruthoff, J. Am. Chem. Soc. **92** (1970) 5413.
10. W. A. Pryor and K. Smith, J. Am. Chem. Soc. **92** (1970) 5403.
11. R. C. Neuman and J. V. Behar, J. Am. Chem. Soc. **91** (1969) 6024.
12. R. C. Neuman and M. J. Amrich, J. Am. Chem. Soc. **94** (1972) 2730.
13. C. Rüchardt, Angew. Chem. **82** (1970) 845.
14. T. Komai, K. Matsuyama, and M. Matsushima, Bull. Chem. Soc. Jpn. **61** (1988) 1641.
15. G. Luft, P. Mehrling, and H. Seidl, Angew. Makromol. Chem. **73** (1978) 95.
16. P. Mehrling, G. Luft, B. Giese, and H. Seidl, Chem. Ber. **118** (1985) 240.
17. a) M. Buback and H. Lendle, Z. Naturforsch., Part A **34 a** (1979) 1482; b) M. Buback and S. Klingbeil, Chem. Ing. Tech. **67** (1995) 493; c) M. Buback and C. Hinton, in *High-pressure Techniques in Chemistry and Physics: A Practical Approach*,

W. B. Holzapfel and N. S. Isaacs (Eds.), Oxford University Press, Oxford, New York, Tokyo (1997) 151; d) M. Buback and C. Hinton, Z. Phys. Chem. **193** (1996) 61.
18. M. Buback, D. Nelke, and H. P. Vögele, to be published.
19. M.-B. Sderra, Studienarbeit, Göttingen (1997).
20. M. G. Evans, M. Polanyi, Trans. Faraday Soc. **34** (1938) 11.
21. P. S. Engel, A. I. Dalton, and L. Shen, J. Org. Chem. **39** (1974) 384.
22. J. Sandmann, PhD Thesis, Göttingen (2000).
23. S. W. Benson, *Thermochemical Kinetics*, 2nd Edition, Wiley Interscience Publications, John Wiley and Sons, New York, London, Sydney, Toronto (1976).
24. C. Walling, in *Energetics of organic free radicals*, Vol. 4, J. Simoes, A. Greenberg, J. Liebmann (Eds.), Blackie, London (1996) ISBN 0-7514-0378-4.
25. J. D. Cox and G. Bilcher, *Thermochemistry of Organic and Organometallic Compounds*, Academic Press, London, New York (1970).
26. B. Abel, J. Assmann, M. Buback, M. Kling, S. Schmatz, and J. Schroeder, Angew. Chem. Int. Ed. **42** (2003) 299.